

# Diameter Effect on the Propagation of Curved Detonation Waves in Micro-Channel Charges Within a Strong Confinement

Qingjie Jiao,<sup>[a]</sup> Haitong Song,<sup>[a, b]</sup> Jianxin Nie,<sup>\*[a]</sup> Rongqiang Liu,<sup>[a]</sup> Xinchun Xu,<sup>[c]</sup> and Yuquan Wen<sup>[a]</sup>

**Abstract:** The property of detonation wave propagation in micro-channel charges is one of the most important research areas in the field of explosives. Based on DSD (Detonation Shock Dynamics) theory and a linear assumption for the streamline deflection angle, this paper proposes a theoretical model for curved detonation wave propagation in cylinder-type micro-channel charges within a strong confinement of metal tube. Further, dynamic control equations related to the detonation velocity and charge diameter are deduced, a numerical calculation method of detonation velocity and shock front shape is given, and propagation rules for detonation waves with different diameters are obtained.

An experiment was designed to test the detonation velocities for micro-channel charges with a booster explosive. The results closely agree with calculations, validating the propagation model of curved detonation waves. It was found that the detonation velocity loss and shock front curvature in the central axis decreased with increasing diameter in the calculation range. Moreover, the smaller the diameter, the greater the rate of change. It is also shown that the model is suitable for the prediction of diameter effects in micro-channel charges, which is of significance for structural design and performance optimization in MEMS initiation systems.

**Keywords:** curved detonation wave · propagation · diameter effect · micro-channel

## 1 Introduction

During the last 10 years, many countries have invested in micro-spacecraft, microsatellites, and micro-explosive devices as important development directions in the field of space exploration. The attitude control, ignition and separation, orbit correction and safety insurance of these digital, intelligent devices are inseparable from the micro-ignition sequence and micro-detonation system based on MEMS (Micro-Electro-Mechanics System) technology [1,2]. The performance of MEMS initiation devices, as the starting point of the whole energy transfer system, is closely related to the safety and the reliability of aerospace equipment. Generally, the charge diameter of micro-explosives in MEMS is in the millimeter range but, because of the diameter effect [3], detonations tend to propagate significantly below the nominal one-dimensional detonation speed. Detonation velocity in micro-channel explosives depends not only on the size of the charge but also on confinement. Modeling of the propagation process is difficult due to a lack of first-principle understanding in the coupling mechanisms of these effects in micro-channel charges.

There have been many previous studies to investigate the diameter effect in detonation wave propagation. Campbell [4] *et al.* measured the diameter-effect curve of explosive PBX-9502 (95 wt.% TATB, 5 wt.% Kel-F 800) at different temperatures and found that temperature can affect the critical diameter for small sizes of charge. Jette [5] *et al.*

analyzed the effect of reaction rate and lateral losses on the critical diameter for small sized charges based on experimental data, finding that the critical radius is strongly dependent on the value of the parameter in the reaction rate equation and that a stiff confinement material can help reduce the critical radius. Tran [6] *et al.* found that a detonation wave is closely related to charge diameter and density through experiment and the confinement material can affect the detonation velocity and shock front curvature. In recent years a discrete Boltzmann model, or lattice Boltzmann kinetic model, was proposed to investigate the non-equilibrium effects in combustion systems, especially in micro-channel explosion systems [7–10]. Further, much numerical simulation work has been done on detonation wave propagation to study the diameter effect. Lefrancois [11] *et al.* applied LS-DYNA software to determine the critical transmission diameter of explosive LX-16 (96 wt.% PETN,

[a] Q. Jiao, H. Song, J. Nie, R. Liu, Y. Wen  
State Key Laboratory of Explosion Science and Technology, Beijing  
Institute of Technology, No. 5, Zhongguancun South Street, Haidian  
District, Beijing, China  
\*e-mail: niejx@bit.edu.cn

[b] H. Song  
713th research institute of China shipbuilding industry corporation,  
Zhengzhou, China

[c] X. Xu  
Beijing Power Machinery Research Institution, Beijing, China

4 wt.% FPC 461) through the ignition growth model and analyzed the optimal constraint conditions. Chinnayya [12] *et al.* carried out a numerical study of propagation for regular detonation waves in the context of narrow channels undergoing strong wall confinement, and analyzed the effect of streamline divergence and wall dissipation on main energy withdrawals and detonation velocity. Sow [13] *et al.* discussed the influence of friction and heat losses on the propagation of one-dimensional detonation waves based on numerical simulation, and Bao [14] *et al.* analyzed the output pressure of JO-9C (95 wt.%HMX, 5 wt.% Viton) explosives with a series of small diameters by combining experimental tests and numerical simulations. For a water gap test to characterize the shock sensitiveness of small confined explosive components, Lefrancois [15] *et al.* investigated the influence of a number of experimental parameters on the go-no go threshold by using LS-DYNA software, and concluded that the possible explanation of the go-no go threshold drop is certainly the double shock desensitization mechanism. Roeske [16] *et al.* studied the corner effect of the detonation wave in an HMX-based explosive and found that the distance the detonation wave has to travel past the turn in order to regain its original symmetry is governed by an exponential time constant of 0.6  $\mu\text{s}$ .

The diameter effect is due to the propagation of radial release waves from the charge side surface to the detonation reaction zone. The confinement effect of the inert medium can reduce the release waves on the propagation of the detonation wave. Therefore, the propagation of detonation waves in micro-channel charges is determined by nonlinear couplings between multidimensional effects and chemical kinetics, which makes the theoretical research very complex. Watt [17] *et al.* studied the detonation velocities in detonation wave propagation by approximating the streamline in straight lines, but the result was found to be better when the charge was unconstrained. Xu [18] *et al.* studied the detonation velocities of detonation waves in micro-channel explosives, but it was assumed that the curved detonation wave front is flat, which is not true. However, none of the above provided a comprehensive description of the non-ideal detonation behavior in micro-channel charges within a strong confinement.

Jackson [19] *et al.* conducted experiments to characterize the detonation phase-velocity dependence on charge thickness for two-dimensional detonation in condensed-phase explosive slabs and charge radius in condensed-phase explosive cylinder, and found that the ratio of cylinder radius ( $R$ ) to slab thickness ( $T$ ) at each detonation phase velocity ( $D_0$ ) is such that  $R(D_0)/T(D_0) < 1$ , and explained the phenomenon with the Detonation Shock Dynamics (DSD) theory. The DSD theory [20,21] has proven very successful for weak non-ideal detonations. The theory shows that the normal detonation velocity is closely related to the local shock front curvature, causing widespread concern. Short [22] *et al.* studied the stable propagation law of detonation waves in circular arcs based on DSD theory and obtained

the relation between detonation propagation angular velocity and arc diameter, thickness, and constraint conditions. Yoo [23] studied the detonation mechanism of heterogeneous explosives using hydrodynamic simulations and obtained the relationship between normal detonation velocity and the shock front curvature, which is in good agreement with DSD theory. These all show that DSD theory can provide a good description of curved detonation waves in non-ideal detonations. However, theoretical analysis of the diameter effect for propagation of detonation waves in micro-channel charges with strong confinement has yet to be investigated using DSD theory.

Starting from classical DSD theory, this paper considers the radial sparse wave and confinement effect based on reasonable physical assumptions. Then the propagation model, control equations and numerical calculation method for curved detonation waves in micro-channel charges within a strong confinement were obtained. Furthermore, the wave propagation rules caused by the diameter effect were obtained. Finally, we designed an experiment to test the detonation velocities for micro-channel charges with a booster explosive and compared the calculated data with the experimental results, which were in good agreement and validated the propagation model of curved detonation waves.

## 2 Mathematical Model and Analysis Process

As shown in Figure 1, the micro-channel charge mainly consists of an explosive charge and inert metal material. The charge is cylindrical with diameter  $d$ , and the outer diameter of the confinement tube is  $d_0$ . During the following theoretical analysis process, we assumed that the outer strong confinement tube is thick enough than the micro-channel charge, which could greatly simplify our mathematical model without taking into account the confinement thickness.

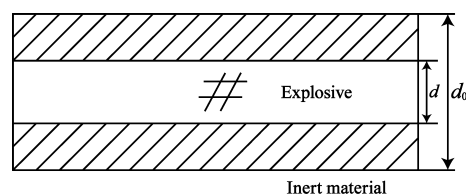
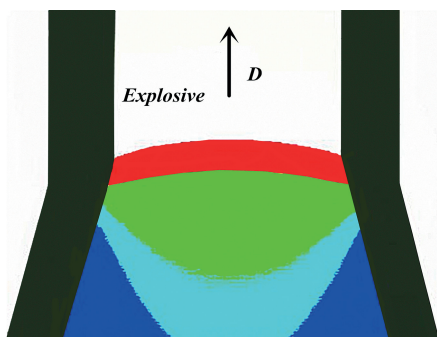


Figure 1. Physical model for the micro-channel charge.

A detonation wave consists of a lead shock front followed by a thin exothermic chemical reaction zone. In the process of steady non-ideal detonation, because of the influence of lateral sparse waves, the response of energy from the reaction zone to the shock front is weaker than that of ideal detonation. The detonation shock front is curved, and the streamlines behind the detonation shock front diverge. Figure 2 shows a schematic of steady non-ideal detonation.



**Figure 2.** Schematic of steady non-ideal detonation with a strong confinement.

A coordinate system for the shock front was established, as shown in Figure 3, with the reference coordinate system origin at the intersection of the shock front and the inert material;  $y$  is the direction of propagation of the detonation and  $x$  is the radial direction toward the central axis. The detonation wave propagates forward at velocity  $D$  along the  $y$ -axis direction, where  $\theta$  is the streamline deflection angle,  $\varphi$  is the angle between the shock front and the  $y$ -axis, and  $\theta_0$  is the streamline deflection angle at the boundary, which is also the deformation angle of the inert material caused by the bow shock induced by the detonation wave.

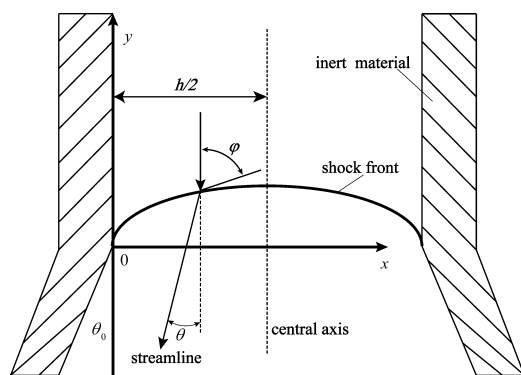


**Figure 3.** Coordinate system for shock front.

The shape of the shock front is represented by the function  $y_f = y_f(x_f)$ . In this study, the diameter of the micro-channel charge studied is in millimeters, and the deformation angle of the inert material is small; therefore, it was assumed that the streamline deflection angle varies linearly along the shock front from the boundary to the central axis. From these conditions;

$$y'_f = dy_f/dx_f = \cot \varphi \quad (1)$$

$$\theta = \theta_0 \left( 1 - \frac{2x_f}{d} \right) \quad (2)$$

From the deflection angle relationship on the shock front [24], the following can be obtained;

$$\tan \theta = \frac{\cot \varphi}{\gamma + (\gamma + 1) \cot^2 \varphi} \quad (3)$$

where  $\gamma$  [25] is the entropic index of the detonation products.

Eq. (3) can be combined with Eqs. (1) and (2) to yield the shock front function;

$$(\gamma + 1) \tan \left[ \theta_0 \left( 1 - \frac{2x_f}{d} \right) \right] y_f'^2 - y_f' + \gamma \tan \left[ \theta_0 \left( 1 - \frac{2x_f}{d} \right) \right] = 0 \quad (4)$$

where the boundary conditions are:  $x_f = 0$ ,  $y_f = 0$  and  $x_f = d/2$ ,  $y_f' = 0$ .

According to Xu's [16] expanding model for micro-channel charges, the boundary angle was studied. In the early stages, when the confinement is expanded by the high pressure in the reaction zone, the interface produced a shock spreading along the radial direction within the confinement while a fan of refracted waves is reflected to the reaction zone along the radial direction. Suppose the state of the reaction zone is approximately the state of the end plane of the reaction zone, and the reflected refraction waves are approximately a weak shock wave then, according to momentum equation.

For confinement:

$$p_m = \rho_{m0} D_m u_m \quad (5)$$

For detonation products:

$$p_r - p_j = -\rho_j C_j u_r \quad (6)$$

Continuity condition at the interface:

$$p_m = p_r, u_m = u_r \quad (7)$$

Combining Eqs. (5) and (6) with (7) gives:

$$u_m = \frac{p_j}{\rho_{m0} D_m + \rho_j C_j} \quad (8)$$

where  $p_m$  is the pressure in the inert material,  $\rho_{m0}$  is the initial density of the inert material,  $D_m$  is the shock wave velocity in the inert material,  $u_m$  is the particle velocity in the inert material,  $p_r$  is the pressure of the detonation products at the interface,  $p_j$  is the pressure of the detonation reaction zone,  $\rho_j$  is the density of the detonation reaction zone,  $C_j$  is the velocity of the reflected weak shock wave, and  $u_r$  is the radial expansion velocity of the products.

According to the Hugoniot relationship of a confinement material:

$$D_m = a_m + b_m u_m \quad (9)$$

where  $a_m$  and  $b_m$  are the Hugoniot parameters related to the solid material.

The density of the explosive charge is  $\rho_0$ . According to the classical C–J formula,

$$p_j = \frac{1}{\gamma + 1} \rho_0 D^2, \quad \rho_j = \frac{\gamma + 1}{\gamma} \rho_0, \quad C_j = \frac{\gamma}{\gamma + 1} D, \text{ hence;}$$

$$\theta_0 = \arctan \frac{u_m}{D} = \arctan$$

$$\frac{2D}{(\gamma + 1) \left[ am\eta + D + \sqrt{(am\eta - D)^2 + 4\eta \left( amD - \frac{bmD^2}{\gamma + 1} \right)} \right]} \quad (10)$$

where  $\eta = \rho_{m0}/\rho_0$ .

The normal detonation velocity is linearly related to the local shock front curvature according to DSD theory [13, 14];

$$\frac{D_n}{D_j} = 1 - \alpha \kappa \quad (11)$$

$$\kappa = \frac{|y_f''|}{(1 + y_f'^2)^{3/2}} + \frac{y_f'}{x_f \sqrt{1 + y_f'^2}} \quad (12)$$

where  $D_n$  is the normal detonation velocity on detonation shock front,  $D_n = D \cdot \sin(\varphi)$ ,  $D_j$  is the ideal one-dimensional detonation velocity,  $\kappa$  is local mean curvature at  $x_f$  on detonation shock front, and  $\alpha$  is a parameter to characterize the sensitivity of normal detonation velocity to the shock front curvature.

Differentiating Eqs. (1), (2), and (3);

$$y_f'' = \left( \frac{2\theta_0}{d \cos^2 \theta} \right) \frac{[\gamma + (\gamma + 1) \cot^2 \varphi]^2}{[(\gamma + 1) \cot^2 \varphi - \gamma]} \quad (13)$$

When  $x_f = d/2$ ,  $\theta = 0$ ,  $\varphi = \pi/2$ , and  $y_f' = 0$  which, when combined with Eqs. (7), (8), and (9), yield:

$$\frac{D}{D_j} = 1 - \alpha \frac{2\gamma\theta_0(D)}{d} \quad (14)$$

In this way, Eqs. (10) and (14) can be used to solve the detonation velocity in the process of detonation wave propagation in micro-channel charges within confinement. The equations are nonlinear, and an analytic solution of detonation velocity  $D$  cannot be given. Therefore, iterative calculations were carried out by a numerical solution method. The iterative formula is:

$$D_{i+1} = D_j \left[ 1 - \alpha \frac{2\gamma}{d} \theta_0(D_i) \right] \quad (15)$$

A matlab program was written to calculate each equa-

tion, where  $\delta$  is the calculation accuracy,  $n$  is the number of cycles, and  $N$  is the maximum number of cycles. The calculation flow chart is shown in Figure 4.

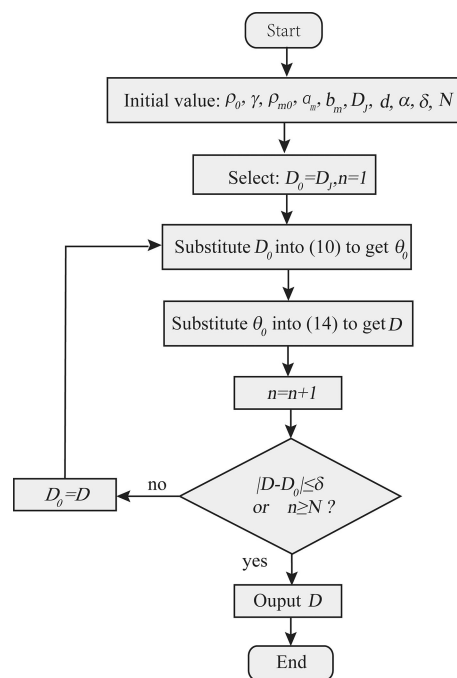


Figure 4. Schematic of the calculation flow chart.

## 3 Experiment and Results

In this paper, we designed an experiment to measure the detonation velocity in micro-channel charge within a strong confinement, and compared the calculated data with the experimental results. For each round of testing, the sample was consisted of four sections of 20 mm outer-diameter tubes with pressed high explosives. The length of the first section is 25 mm and that of each remaining three ones is 10 mm, which can ensure that the detonation wave in the last three micro-channel charges grows to the stable propagation stage during the experiment. The explosive used in the experiment was fine particles of JO-9C (a new insensitive booster explosive based on HMX), and the confinement material was steel. In order to avoid the charge density gradient, a step-by-step press fitting technology was applied to make micro-channel explosive samples. Characteristics of the high explosives and charge sizes are given in Table 1, and the steel cartridge and explosive cylinder are as shown in Figure 5.

The electric probe method was used to measure detonation velocities of micro-channel charges in the experiment. Three pairs of the probe were sandwiched among four sections with high explosive. The basic principle of measuring technology in this test is: to utilize conductive ions of the detonation wave front, three pulse signals will

**Table 1.** Characteristics of high explosives and charge sizes.

| Explosive | Proportion of components (wt.%) | Density (g cm <sup>-3</sup> ) | Charge diameter (mm) |
|-----------|---------------------------------|-------------------------------|----------------------|
| JO-9C     | HMX/Viton 95%/5%                | 1.707                         | 0.9                  |
|           |                                 |                               | 1.5                  |
|           |                                 |                               | 2                    |
|           |                                 |                               | 3                    |
|           |                                 |                               | 4                    |
|           |                                 |                               | 5                    |



**Figure 5.** Image of: (a) steel cartridge and (b) completed explosive cylinder.

be produced while the detonation wave propagates through four electric probes in turn. Two time intervals of detonation wave traveling through three probes can be exactly measured, and then the average detonation velocity will be easily calculated by dividing the two-probe distance by the average time interval. The main working flow of testing detonation velocity is as follows: A DC power supply was used to detonate an 8# industrial electric detonator, which then detonates the charge. In the propagation process, the detonation wave turns on the trigger probe. The probe signal was converted by a multi-channel program-controlled signal generator and was then recorded by a 32-channel time-interval measuring instrument. Finally, the results were printed. Figure 6 shows a schematic diagram of the overall experimental configuration. For each condition of different charge diameter, three-round tests were performed to ensure the reproducible measured results of detonation wave velocity. The measuring deviation of deto-

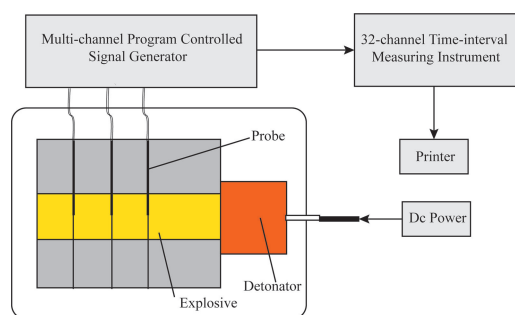


**Figure 6.** Schematic diagram of the experimental setup.

nation velocities ranges from 3.28% to 10.40%. The test results for detonation velocities with different charge diameters are shown in Table 2.

**Table 2.** Experimental data of detonation velocity.

| Confinement | Diameter/mm | Time interval/ $\mu$ s | Experimental $D$ /mm/ $\mu$ s |
|-------------|-------------|------------------------|-------------------------------|
| Steel       | 0.9         | 1.510                  | $6.622 \pm 0.054$             |
| Steel       | 1.5         | 1.445                  | $6.922 \pm 0.072$             |
| Steel       | 2           | 1.325                  | $7.547 \pm 0.052$             |
| Steel       | 3           | 1.302                  | $7.680 \pm 0.061$             |
| Steel       | 4           | 1.279                  | $7.820 \pm 0.033$             |
| Steel       | 5           | 1.259                  | $7.940 \pm 0.026$             |

## 4 Calculated Results and Comparison

Based on the proposed propagation model of curved detonation waves in micro-channel charges within a strong confinement, the characteristic parameters of explosive JO-9C, such as detonation velocity, shape of the shock front and the shock front curvature, were calculated. The standard values of  $\gamma = 2.67$  and  $D_j = 8.46 \text{ mm} \cdot \mu\text{s}^{-1}$  were used. The value of  $\alpha$  is related to the intrinsic properties of the explosive. It is usually calibrated by observing the wave front shape. Zhang [26] carried out an experiment and found the  $\alpha$  value of HMX/TNT for ratios of 60/40 and 50/50 were 0.9 mm and 1 mm. Here  $\alpha$  was designated as 0.6 mm according to previous experience; the detonation velocities for different charge diameters were calculated according to the flow chart Figure 4 and compared with experimental data, as shown in Figure 7. Detonation velocity losses for different diameters were analyzed from the calculated data, as shown in Figure 8. The detonation velocity loss  $\Delta_D$  is defined by the following formula:

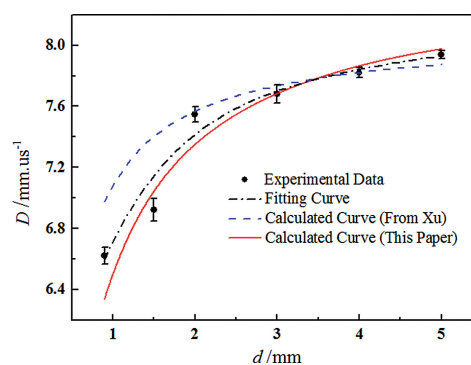


**Figure 7.** Detonation velocity versus diameter. (The calculated results were compared with the experimental results and Xu's [8]).



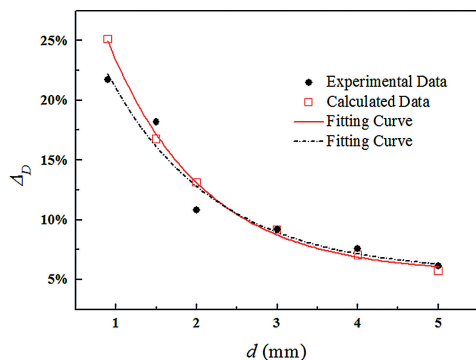


Figure 8. Detonation velocity loss versus diameter.

$$\Delta D = \frac{DJ - D}{DJ} \times 100\% \quad (16)$$

It can be seen from Figure 7 that the calculated results agree closely with the experimental results, with the variation trend being the same. The maximum error is 4.3%, which is better than that of Xu's especially for diameters less than 2 mm. For the propagation model, the effect of a confinement material, lateral sparse wave and the divergence of streamlines were analyzed, thus the propagation model in this paper is in better agreement with experimental data.

In Figure 7, detonation velocity increases with increasing diameter, and the larger the charge diameter is, the smoother the  $D$ - $d$  curves become. The detonation velocity increases rapidly when the diameter increases from 0.9 mm to 2 mm, but changes less rapidly when the diameter increases from 2 mm to 5 mm. It can be seen from Figure 8 that the detonation velocity loss decreases with increasing diameter; when  $d=0.9$  mm the detonation velocity loss is 25% and when  $d=5$  mm the detonation velocity loss is 6%. A smaller diameter corresponds to an improved rate of change of detonation velocity loss. The calculation formula of  $\Delta D$  can be fitted from the calculated data in Figure 8,  $\Delta D = 0.473 - 0.418 (1 - e^{(-d/1.174)})$ , with a relevance of 0.997; this can be used to guide structure design and predict the performance of micro-channel charges.

Considering the confinement effect and linear assumptions for the streamline deflection angle, the shape of the shock front was obtained through numerical calculation with the curved detonation shock front in a non-ideal detonation process being analyzed. As shown in Figure 9, the shock front for micro-channel charges with different diameters were calculated when  $\alpha=0.6$  mm. It was found that the distance of the shock front increases with increasing diameter. As shown in Figure 10,  $\kappa_c$  is the local shock front curvature in the central axis, with the increasing diameter  $\kappa_c$  is decreasing, eventually the changing trend of  $\kappa_c$  versus  $d$  becoming smooth. It was found that  $\kappa_c$  dropped from  $0.4188 \text{ mm}^{-1}$  to  $0.0955 \text{ mm}^{-1}$  as the charge diameter increased from 0.9 mm to 5 mm. As the diameter tends to-

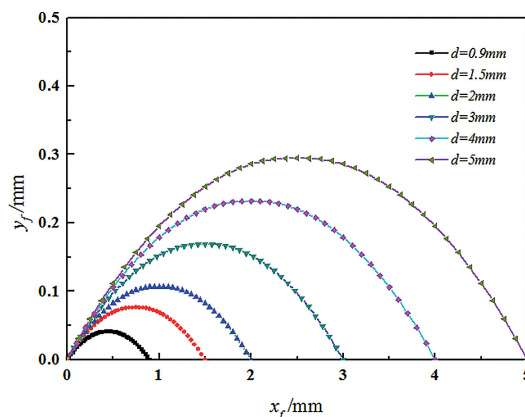


Figure 9. Curved shock front shape versus diameter.

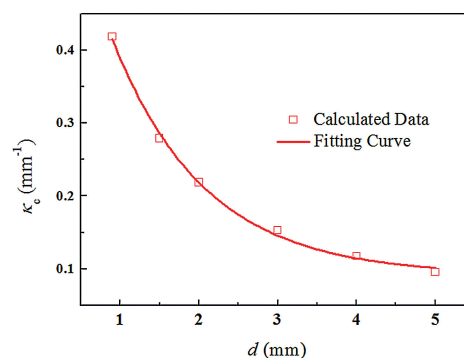
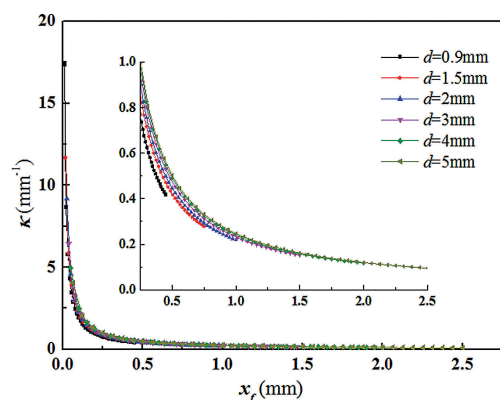


Figure 10. Local curvature of shock front in central axis versus diameter.

wards infinity,  $\kappa_c$  approaches zero, that is, the shock front is close to that of a flat plane. In addition, a smaller diameter corresponds to a significantly improved rate of change for the curvature. The calculation formula of  $\kappa_c$  can be fitted from the calculated data in Figure 10 giving  $\kappa_c = 0.789 - 0.697 (1 - e^{(-d/1.173)})$ , with a relevance of 0.997, which is of significance for mechanism analysis and engineering applications in micro-scale detonation.

For a certain charge diameter condition, the shock front curvature  $\kappa$  at the position of any  $x_f$  could be calculated by combining equations (1) to (4), (13), and (12). In Figure 11, we can see that  $\kappa$  decreases with increasing  $x_f$  and is smallest in the central axis under different charge diameter conditions. Moreover, the closer is the position to the edge of the charge, the larger is the value of  $\kappa$ , which is well consistent with the trend of  $\kappa(r)$  curves in Figure 4 performed by Hill [27] *et al.*

According to the 'diameter effect' and for the process of steady non-ideal detonation, due to the lateral expansion, energy density in the reaction zone, detonation wave strength, and excited chemical reaction rate decrease, this will lead to a decrease in detonation velocity and a bending of the shock front. Therefore, the reaction zone is widened,



**Figure 11.**  $\kappa(x_f)$  curves with different charge diameter conditions.

and, in turn, the detonation intensity is weakened. Such an energy loss cycle results in a smaller charge diameter and a greater impact on the detonation velocity and detonation wave. The principle is in accordance with the results of this study.

## 5 Conclusion

In this paper, a propagation model was established for curved detonation waves in micro-channel charges within a strong confinement based on classic DSD and a linear assumption of the streamline deflection angle. Using a numerical calculation method, the detonation velocities and shapes of the curved detonation shock front for JO-9C with a charge diameter range of 0.9 to 5 mm were obtained; characteristics of the curved shock front and the mechanism were also analyzed. This study is of significance for structural design and performance optimization in MEMS initiation systems. The following conclusions were obtained:

- (1) The effect of confinement materials and lateral sparse wave, and the divergence of streamlines are analyzed resulting in a propagation model of the curved detonation wave in this paper being a better representation of fact. The calculated detonation velocities agreed closely with experimental results.
- (2) The smaller the diameter, the greater the diameter effect in the propagation of the curved detonation wave.
- (3) Within the calculation range, the detonation velocity loss is about 25% when the charge diameter is 0.9 mm and decreases with increasing diameter. When the charge diameter is 5 mm the detonation velocity loss is about 6%.
- (4) Within the calculation range, the local shock front curvature in the central axis drops from  $0.4188 \text{ mm}^{-1}$  to  $0.0955 \text{ mm}^{-1}$  as the charge diameter increase from 0.9 mm to 5 mm, and in total dropped about 77% in the calculation range.

Further investigations are needed to perform experiments to measure the detonation wave curvature, to analyze the detonation wave growth in micro-channel charges, and the influencing factors on the propagation of detonation wave such as different high explosive composition or different initiation.

## Acknowledgements

This work was supported by the National Natural Science Foundation of China (Grant No. 11772058).

## References

- [1] C. Rossi, D. Estève, Micropyrotechnics, a new technology for making energetic microsystems: review and prospective, *Sens. Actuators A* **2005**, *120*, 297–310.
- [2] C. Rossi, D. Estève, N. Fabre, T. Do Conto, V. Conédéra, D. Dilhan, Y. Guélou, A new generation of MEMS based microthrusters for microspacecraft applications, *Proc. Micro-Nanotechnology for Space Applications*, 1999, *1*: 1045–1048.
- [3] B. P. Zhang, Q. M. Zhang, F. L. Huang. *Detonation Physics*, Weapon Industry Press, Beijing, **2001**, p 180. (In Chinese)
- [4] A. W. Campbell, Diameter Effect and Failure Diameter of a TATB-Based Explosive, *Propellants Explos. Pyrotech.* **1984**, *9*, 183–187.
- [5] F. X. Jette, A. J. Higgins, CRITICAL DIAMETER PREDICTION FOR STEADY DETONATION IN GASLESS METAL-SULFUR COMPOSITIONS, *AIP Conf. Proc. AIP* **2007**, *955*, 385–388.
- [6] T. D. Tran, C. M. Tarver, J. Maienschein, P. Lewis, R. Pastrone, R. S. Lee, F. Roeske, *Characterization of detonation wave propagation in LX-17 near the critical diameter*, Report No. UCRL-JC-144957, Lawrence Livermore National Lab, CA (US), **2002**.
- [7] A. Xu, G. Zhang, Y. Ying, Progress of discrete Boltzmann modeling and simulation of combustion system, *Acta Physica Sinica* **2015**, *64*, 184701.
- [8] A. Xu, C. Lin, G. Zhang, Y. Li, Multiple-relaxation-time lattice Boltzmann kinetic model for combustion, *Physical Review E* **2015**, *91*, 043306.
- [9] C. Lin, A. Xu, G. Zhang, Y. Li, Double-distribution-function discrete Boltzmann model for combustion, *Combust. Flame* **2016**, *164*, 137–151.
- [10] Y. Zhang, A. Xu, G. Zhang, C. Zhu, C. Lin, Kinetic modeling of detonation and effects of negative temperature coefficient, *Combust. Flame* **2016**, *173*, 483–492.
- [11] A. Lefrançois, J. Benterou, F. Roeske, *Diameter Effect In Initiating Explosives, Numerical Simulations*, Report No. UCRL-TR-219006, Lawrence Livermore National Lab.(LLNL), Livermore, CA (United States), **2006**.
- [12] A. Chinnayya, A. Hadjadj, D. Ngomo, Computational study of detonation wave propagation in narrow channels, *Phys. Fluids* **2013**, *25*, 036101.
- [13] A. Sow, A. Chinnayya, A. Hadjadj, Effect of friction and heat losses on the mean structure of one-dimensional detonations, *AIP Conf. Proc.* **2013**, *1558*, 140–143.
- [14] B. Bao, N. Yan, F. Zhu, Research on the Influence of Charge Diameter upon the Output Pressure of Small-Sized Explosives, *Cent. Eur. J. Energ. Mater.* **2015**, *12*.
- [15] A. S. Lefrançois, R. S. Lee, C. M. Tarver, Shock desensitization effect in the confined explosive component water gap test de-

- fined by the NATO standardization agreement (STANAG) 4363, *Propellants Explos. Pyrotech.* **2007**, 32, 244–250.
- [16] F. Roeske, P. C. Souers, Corner Turning of Detonation Waves in an HMX-based Paste Explosive, *Propellants Explos. Pyrotech.* **2000**, 25, 172–178.
- [17] S. D. Watt, G. J. Sharpe, S. A. E. G. Falle, M. Braithwaite, A streamline approach to two-dimensional steady non-ideal detonation: the straight streamline approximation, *J. Eng. Math* **2012**, 75, 1–14.
- [18] X. Xu, Q. Jiao, Z. Jin, G. Yang, Confinement Effects and Diameter Effects on the Non-ideal Detonation Parameters of Small Charge, *J. Beijing Inst. Technol. (Engl. Ed.)* **2010**, 19, 399–404.
- [19] S. I. Jackson, M. J. Short, Scaling of detonation velocity in cylinder and slab geometries for ideal, insensitive and non-ideal explosives, *J Fluid Mech.* **2015**, 773, 224–266.
- [20] J. B. Bdzil, Steady-state two-dimensional detonation, *J Fluid Mech.* **1981**, 108, 195–226.
- [21] J. B. Bdzil, D. S. Stewart, Modeling two-dimensional detonations with detonation shock dynamics, *Phys. Fluids A* **1989**, 1, 1261–1267.
- [22] M. Short, J. J. Quirk, C. D. Meyer, C. Chiquete, Steady detonation propagation in a circular arc: a Detonation Shock Dynamics model, *J Fluid Mech.* **2016**, 807, 87–134.
- [23] S. Yoo, M. Crochet, S. Pemberton, Modeling normal shock velocity curvature relations for heterogeneous explosives, *AIP Conf. Proc.* AIP Publishing, **2017**, 1793, 030020.
- [24] B. Dunne, Mach reflection of detonation waves in condensed high explosives. II, *Phys. Fluids* **1964**, 7, 1707–1712.
- [25] D. S. Stewart, S. Yoo, W. C. Davis, Equation of state for modeling the detonation reaction zone, *12th Symp.(Intl) on Detonation* **2002**, 1–11.
- [26] H. Zhang, F. Huang, Study on the Dn(k) relation for the RDX/TNT and HMX/TNT rate sticks, *Explosion and Shock Waves* **2012**, 32, 495–500. (In Chinese)
- [27] L. G. Hill, J. B. Bdzil, T. D. Aslam, *Front curvature rate stick measurements and detonation shock dynamics calibration for PBX 9502 over a wide temperature range*, 11th Symp.(Intl) on Detonation, **1998**. 1–9.

Received: February 11, 2018  
Published online: July 2, 2018